Eur. Phys. J. B **7**, 211–218 (1999)

THE EUROPEAN PHYSICAL JOURNAL B

EDP Sciences

Van der Waals interaction between flux lines in high-T_c superconductors: A variational approach

A. Volmer[1,a] and M. Schwartz[2]

[1] Universität zu Köln, Institut für theoretische Physik, Zülpicher Str. 77, 50937 Köln, Germany
[2] Tel Aviv University, The Raymond and Beverly Sackler Faculty of Exact Sciences, School of Physics and Astronomy, 69978 Tel Aviv, Israel

Received: 25 June 1996 / Revised: 18 August 1998 / Accepted: 21 August 1998

Abstract. In pure anisotropic or layered superconductors thermal fluctuations induce a van der Waals attraction between flux lines. This attraction together with the entropic repulsion has interesting consequences for the low field phase diagram; in particular, a first order transition from the Meissner phase to the mixed state is induced. We introduce a new variational approach that allows for the calculation of the effective free energy of the flux line lattice on the scale of the mean flux line distance a, which is based on an expansion of the free energy around the regular triangular Abrikosov lattice. Using this technique, the low field phase diagram of these materials may be explored. The results of this technique are compared with a recent functional RG treatment of the same system.

PACS. 74.60.Ec Mixed state, critical fields, and surface sheath – 74.72.Hs Bi-based cuprates

1 Introduction

The physics of flux lines in high-T_c superconductors at low magnetic fields is dominated by the short ranged bare repulsion between flux lines and a long ranged entropic repulsion due to thermal fluctuations. This results in a first order melting transition from the Abrikosov lattice [1] to a liquid phase close to the lower critical field H_{c_1}, as has been predicted some time ago by Nelson [2]. For mean flux line distances, a, larger than the London penetration depth λ, the bare interaction decays exponentially with a, while the entropic repulsion decays algebraically $\sim(\lambda^2/L_T a)^2$. Here, the thermal length scale $L_T = \Phi_0^2/(16\pi^2 T) \approx 2/T\,\mathrm{cm\,K}$ denotes the length of an isolated flux line segment that shows a thermal mean square displacement of the order of λ [3], and $\Phi_0 = hc/2e$ is the flux quantum carried by each flux line. Close to the transition to the Meissner phase, the entropic repulsion dominates over the bare interaction, leading to a magnetic induction B that vanishes linearly with the reduced field strength $\tilde{h} = (H - H_{c_1})/H_{c_1}$ [2].

In strongly anisotropic or layered superconductors an additional interaction between flux lines has been found recently by Blatter and Geshkenbein (BG) [4]: in the situation where the applied magnetic field is perpendicular to the CuO layers, short scale fluctuations on the scale of pancake vortices lead to an *attractive* van der Waals (vdW) interaction. (This is in fact also the origin of the long range attraction of a flux line to the surface [5].) For flux lines separated by a distance R the strength of this interaction is of the order $-\lambda^6/(dL_T R^4)$ for $\lambda < R < d/\varepsilon$ and $\simeq -\lambda^6/(\varepsilon L_T R^5)$ for $d/\varepsilon < R < \lambda/\varepsilon$. Here, $\varepsilon^2 = m/M \ll 1$ denotes the anisotropy of the material with m and M the effective masses parallel and perpendicular to the CuO_2 plane, respectively, and d the interlayer spacing. Apart from this thermally induced attraction, also frozen-in disorder in impure superconductors induces an attraction between flux lines with the same dependence on the distance R [7,8]. This disorder induced attraction dominates at very low temperature $T \ll T_{dis}$, where T_{dis} depends on the disorder strength [3]. Here, we will focus on the opposite case $T \gg T_{dis}$ where it is sufficient to consider thermal fluctuations.

The competition among the bare, the entropic and the vdW interactions leads to an interesting phase diagram at low B values. In particular, the vdW attraction can lead to an instability of the Abrikosov lattice in the dilute limit $a \gg \lambda$, resulting in a first order transition between the Meissner and the mixed phase [4].

In order to calculate the low B phase diagram of pure layered high-T_c superconductors, one has to calculate the Gibbs free energy density of this system on the scale of the mean flux line distance a,

$$g(a; H, T) = f(a, T) - \frac{\varepsilon_o \ln\kappa}{a^2}\,\tilde{h}, \tag{1}$$

which has to be minimized with respect to a with the external magnetic field H fixed. Here, $f(a,T)$ is the free energy density, $\varepsilon_o = (\Phi_0/4\pi\lambda)^2 = L_T T/\lambda^2$ is the basic

[a] e-mail: av@thp.uni-koeln.de

energy scale, and κ is the Ginzburg-Landau parameter. Note that the bare lower critical field (in the absence of thermal fluctuations) is given by $H_{c_1}^0 = 4\pi\varepsilon_o \ln\kappa/\Phi_0$, and that the magnetic flux is related to the flux line distance *via* $B \simeq \Phi_0/a^2$.

It is the aim of the present paper to propose a new variational approach to obtain this effective Gibbs free energy density, based on a perturbative expansion in small displacements of the flux lines around the regular triangular lattice. This expansion is justified only if we assume that the lattice is stable, *i.e.*, that we are above the lower melting line below which the flux lines form a liquid. The variational technique allows for a check of this assumption by virtue of a Lindemann criterion where the self-consistently determined flux line fluctuations are compared with the mean flux line distance a.

In order to motivate our efforts, let us shortly review the approaches that have been followed so far. In their first paper [4], BG simply added the bare vdW energy, evaluated on the scale a, to the free energy which contains the bare and the entropic repulsion mentioned above. In this way, only contributions from the vdW energy on the length scale a are taken into account, which bears the risk of a gross underestimation of its influence because of its rapid decay for $R > \lambda$. In a subsequent publication [6], BG showed that in the liquid phase, rather the average of the potential over all distances is relevant, as it appears in the usual virial expansion of the vdW gas. Using this technique, one obtains the correct scaling of the vdW contribution to the free energy with the mean FL distance.

In [7], only the dominant contribution from the vdW attraction on the scale R_{min} was taken into account within a scaling approach, where R_{min} is the position of the global minimum of the bare potential $V(R)$. This scaling approach is elegant and simple and yields the correct qualitative picture, but does not allow for quantitative predictions. More recently a functional renormalization group (RG) calculation has been adapted to the same problem [8]; in particular, the low field phase diagram of $Bi_2Sr_2CaCu_2O_x$ (BiSCCO) was calculated. In that approach, the bare flux line interaction is renormalized by thermal fluctuations on all scales between λ and a, providing an effective free energy on the scale of a. The problem in this latter method is that the largest scale up to which fluctuations are taken into account is arbitrary to some extent; we will see below that this flaw is overcome in a natural way by the technique that we will develop below.

The paper is organized as follows: in Section 2 the variational method is set up for arbitrary bare flux line interactions. The method is applied to a flux line lattice in a layered high-T_c superconductor in Section 3. There, the flux line interaction is modeled by the superposition of the bare, short range repulsion and the long range van der Waals attraction, using physical parameters typical for BiSCCO. The data for the free energy obtained there are used for the minimization of the Gibbs free energy density in Section 4. We shortly review the functional RG approach in Section 5 and compare the two methods. Conclusions are drawn in Section 6.

2 Variation of the free energy

Consider a system with N times M flux lines (FLs) in $D = 3$ dimensions, confined to a box of base area L^2 and height $L_\parallel$. (We assume that the applied magnetic field and hence the flux lines are oriented perpendicular to the CuO layer structure.) The equilibrium position of line number (n, m) is given by $\mathbf{R}_{n,m} = n\,\mathbf{a}_1 + m\,\mathbf{a}_2$, where $a = |\mathbf{a}_1| = |\mathbf{a}_2|$ is the mean distance between the FLs. Since in equilibrium the FLs form a triangular lattice we choose

$$\mathbf{a}_n = a\,(\cos(\phi_n)\,\mathbf{e}_x + \sin(\phi_n)\,\mathbf{e}_y), \quad \phi_n = \frac{\pi}{12} + n\frac{\pi}{3}\cdot \quad (2)$$

For $n = 1, \ldots, 6$ these $\mathbf{a}_n$ are the distance vectors $\mathbf{R} - \mathbf{R}'$ for all nearest neighbors $\mathbf{R}'$ of $\mathbf{R}$ on a triangular lattice; note that only the first two of these distance vectors have been used in our parametrization of $\mathbf{R}_{n,m}$. With this definition of the vectors $\mathbf{a}_n$ the equivalence of the x and the y direction is ensured. This results in the simple form for the matrix $K^{\alpha\beta}(\mathbf{q})$ defined below.

We write the actual position of line (n, m) at height z as

$$\mathbf{r}_{n,m}(z) = \mathbf{R}_{n,m} + \mathbf{u}_{n,m}(z). \quad (3)$$

The interaction between the vortices (n, m) and (n', m') is described by the function $V(r(z))$ that depends on the distance at equal height z. We have made the usual assumption that the vortex coordinates vary slowly with z, so that the FL interactions are well approximated by a potential which is local in z; this approximation is only strictly valid when the vortices are parallel to z.

The system is governed by the Hamiltonian

$$H = \frac{\kappa}{2}\int_0^{L_\parallel} dz \sum_{n=1}^{N}\sum_{m=1}^{M} \left(\partial_z \mathbf{u}_{n,m}(z)\right)^2 + \frac{1}{2}\int_0^{L_\parallel} dz \sum_{(n,m)\neq(n',m')} V(\mathbf{r}_{n,m}(z) - \mathbf{r}_{n',m'}(z)). \quad (4)$$

This description of a FL lattice applies in the limit of fluctuations on scales larger than λ, with a non-dispersive line tension $\kappa = \varepsilon_l(k_z \ll 1/\lambda)$; on smaller scales, the FL tension $\varepsilon_l(k_z)$ in anisotropic superconductors is in fact highly dispersive [9]. The FL interaction $V(R)$ will be specified in Section 3; the following treatment makes no assumptions about its specific form.

Applying periodic boundary conditions in all 3 spatial directions (in particular $\mathbf{u}_{n+N,m} = \mathbf{u}_{n,m}$ and $\mathbf{u}_{n,m+M} = \mathbf{u}_{n,m}$), equation (4) can be rewritten in Fourier space as

$$H = \frac{\kappa}{2}\sum_{\mathbf{q}} q_z^2\,|\tilde{\mathbf{u}}(\mathbf{q})|^2 + \int_0^{L_\parallel} dz \sum_{(n,m)\neq(n',m')} \int d^2k \times \tilde{V}_{\mathbf{k}} e^{i\mathbf{k}\cdot(\mathbf{R}_{n,m} - \mathbf{R}_{n',m'} + \mathbf{u}_{n,m}(z) - \mathbf{u}_{n',m'}(z))}. \quad (5)$$

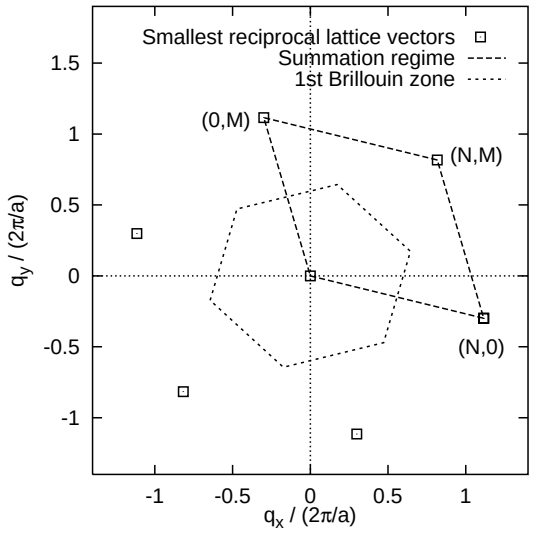

Fig. 1. First Brillouin zone and summation area in $\mathbf{q}_\perp$-space. The vectors $\mathbf{q}_\perp$ with $(n,m) = (N,0)$, $(0,M)$ and (N,M) as defined in equation (6) are reciprocal lattice vectors.

The wave vector q_z takes the discrete values $0, 2\pi/L_\parallel, \ldots, \Lambda$. The ultra violet cutoff Λ has to be introduced explicitly in order to avoid a divergence of the free energy. For the discrete set of $\mathbf{q}_\perp = (q_x, q_y)$ vectors that are summed over, we choose

$$\mathbf{q}_\perp = \frac{2}{\sqrt{3}}\frac{2\pi}{a}\begin{pmatrix} \frac{n}{N}\cos(\pi/12) - \frac{m}{M}\sin(\pi/12) \\ \frac{m}{M}\cos(\pi/12) - \frac{n}{N}\sin(\pi/12) \end{pmatrix}, \quad (6)$$

with $n = 0, \ldots, N-1$ and $m = 0, \ldots, M-1$. This is equivalent to choosing the $\mathbf{q}_\perp$ vectors from the first Brillouin zone (in the 2-dimensional plane perpendicular to the field direction). The summation area in Fourier space, together with the first Brillouin zone, is illustrated in Figure 1.

The Fourier transform of the fluctuating field $\mathbf{u}_{n,m}(z)$ is defined as

$$\tilde{\mathbf{u}}(\mathbf{q}) = \frac{1}{\sqrt{NML_\parallel}}\int_0^{L_\parallel} dz \sum_{n,m} \mathbf{u}_{n,m}(z) e^{-i\mathbf{q}_\perp\cdot\mathbf{R}_{n,m} - iq_z z}, \quad (7)$$

and the Fourier transform of the potential $V(r)$ as $\tilde{V}_\mathbf{k} = \int d^2x\, V(\mathbf{x})\, e^{-i\mathbf{k}\cdot\mathbf{x}}$.

Now, we define a Gaussian variational Hamiltonian

$$H_0 = \frac{1}{2}\sum_\mathbf{q} K^{\alpha\beta}(\mathbf{q})\tilde{u}_\alpha(\mathbf{q})\tilde{u}_\beta(-\mathbf{q}), \quad (8)$$

with summation over the Cartesian components $\alpha, \beta = 1, 2$, and rewrite the original Hamiltonian as

$$H = H_0 + (H - H_0). \quad (9)$$

Let $\langle \ldots \rangle_0$ denote thermal averages with respect to H_0. Clearly,

$$\langle u_\alpha(\mathbf{q}) u_\beta(\mathbf{q}')\rangle_0 = k_B T\, \delta^3_{\mathbf{q}+\mathbf{q}'}\, \tilde{K}^{\alpha\beta}(\mathbf{q}), \quad (10)$$

where $\tilde{K}(\mathbf{q})$ is the Matrix inverse of $K(\mathbf{q})$, *i.e.*,

$$K^{\alpha\beta}(\mathbf{q})\tilde{K}^{\beta\gamma}(\mathbf{q}) = \delta_{\alpha\gamma}.$$

The correlation function $K(\mathbf{q})$ is a 2×2 matrix:

$$K(\mathbf{q}) = \begin{pmatrix} K_D(\mathbf{q}) & K_O(\mathbf{q}) \\ K_O^*(\mathbf{q}) & K_D(\mathbf{q}) \end{pmatrix}. \quad (11)$$

While the diagonal terms $K_D(\mathbf{q})$ are real, the off-diagonal part $K_O(\mathbf{q})$ may in principle take on complex values. In a straightforward but tedious calculation it can be shown however that $K_O(\mathbf{q})$ is actually real, too. For completeness, we give the explicit expression for the matrix inverse $\tilde{K}(\mathbf{q})$:

$$\tilde{K}_{D(O)}(\mathbf{q}) = +(-)\,\frac{K_{D(O)}(\mathbf{q})}{K_D^2(\mathbf{q}) - K_O^2(\mathbf{q})}\,. \quad (12)$$

As stated in the introduction, our aim is to minimize the Gibbs free energy density $g(a; H, T)$ as defined in equation (1) as a function of the mean FL separation a. Let us first consider the free energy $F = F(a, T)$. We define an approximate free energy F^* that is obtained by a first order perturbation expansion around F_0, the free energy associated with H_0,

$$F^* = F_0 + \langle H - H_0\rangle_0. \quad (13)$$

It is well-known [10] that for any choice of H_0, F^* is an upper bound on the true free energy F. Therefore minimization of F^* with respect to the parameters defining H_0, $K_D(\mathbf{q})$ and $K_O(\mathbf{q})$, yields the best approximation of its kind, namely H_0 corresponding to the optimal parameters is the best fluctuating lattice Hamiltonian that may be used to describe our physical system. The free energy F_0 is given by

$$\begin{aligned} F_0 &= -\beta^{-1}\ln\int \mathcal{D}[\mathbf{u}]\, e^{-\beta H_0} \\ &= \frac{1}{2\beta}\sum_\mathbf{q} \ln\det(\beta K(\mathbf{q})). \end{aligned} \quad (14)$$

Next, the expectation value $\langle H - H_0\rangle_0$ shall be calculated. To proceed, it is useful to rewrite the last term in the interaction part of (5) using the Fourier representation (7). Then, the averaging can be immediately carried out, leading to

$$\begin{aligned} \langle H - H_0\rangle_0 = \frac{\kappa}{2}\sum_\mathbf{q} q_z^2\, \mathrm{Tr}\,[\,\tilde{K}(\mathbf{q})\,] - L_\parallel NM\frac{\Lambda}{2\pi}k_B T \\ + \frac{L_\parallel NM}{2}\sum_\mathbf{a}\int_\mathbf{k} \tilde{V}_\mathbf{k}\, e^{i\mathbf{k}\cdot\mathbf{a}} \\ \times\exp\left(-\frac{2k_\alpha k_\beta}{NML_\parallel}\sum_\mathbf{q}\sin^2(\mathbf{q}_\perp\cdot\mathbf{a}/2)\tilde{K}^{\alpha\beta}(\mathbf{q})\right). \end{aligned} \quad (15)$$

We restrict the sum $\sum_\mathbf{a}$ to a summation over nearest neighbors, which is a good approximation in the dilute

limit we are interested in; in principle, one can also include next-nearest neighbors, *etc.* For the triangular lattice, it is convenient to choose the 6 vectors $\mathbf{a}_n$ from equation (2), with $n = 1, \ldots, 6$.

In the following, we choose the temperature $k_BT = \beta^{-1}$ as the basic energy scale, and introduce the parameters $\tilde{\kappa} = \beta\kappa$, the reduced potential $v(\mathbf{r}) = \beta V(\mathbf{r})$ and the reduced Hamiltonian $\mathcal{H} = \beta H$. Finally, we replace $\beta K(\mathbf{q})$ by $K(\mathbf{q})$.

The variational parameters $K_D(\mathbf{q})$ and $K_O(\mathbf{q})$ are determined by minimizing F^*:

$$\frac{\partial F^*}{\partial K_{D(O)}(\mathbf{q})} \stackrel{!}{=} 0. \tag{16}$$

This leads to

$$K_D(\mathbf{q}) = \tilde{\kappa} q_z^2 - 2\sum_{\mathbf{a}} \sin^2(\mathbf{q}_\perp \cdot \mathbf{a}/2)\, A_{\mathbf{a}} \tag{17}$$

$$K_O(\mathbf{q}) = -2\sum_{\mathbf{a}} \sin^2(\mathbf{q}_\perp \cdot \mathbf{a}/2)\, B_{\mathbf{a}} \tag{18}$$

where we have defined

$$A_{\mathbf{a}} = \frac{1}{2}\int_{\mathbf{k}} \mathbf{k}^2\, \tilde{v}(\mathbf{k})\, e^{-i\mathbf{k}\cdot\mathbf{a}} e^{-\frac{1}{2}k_\alpha M_{\mathbf{a}}^{\alpha\beta} k_\beta} \tag{19}$$

and

$$B_{\mathbf{a}} = \frac{1}{2}\int_{\mathbf{k}} 2k_x k_y\, \tilde{v}(\mathbf{k})\, e^{-i\mathbf{k}\cdot\mathbf{a}} e^{-\frac{1}{2}k_\alpha M_{\mathbf{a}}^{\alpha\beta} k_\beta}. \tag{20}$$

By comparison with equation (15), the 2×2 matrix $M_{\mathbf{a}}$ is defined as

$$M_{\mathbf{a}}^{\alpha\beta} = \frac{4}{MNL_\parallel} \sum_{\mathbf{q}} \sin^2(\mathbf{q}_\perp \cdot \mathbf{a}/2)\, \langle u_\alpha(\mathbf{q}) u_\beta(-\mathbf{q})\rangle_0, \tag{21}$$

where we have plugged in the representation (10) of the matrix inverse $\tilde{K}(\mathbf{q})$. Again, $M_{\mathbf{a},D}$ and $M_{\mathbf{a},O}$ are the diagonal and off-diagonal terms, respectively. $\tilde{M}_{\mathbf{a}}$ denotes the matrix inverse of $M_{\mathbf{a}}$. Equations (16–21) serve as a self-consistent set of equations for $K(\mathbf{q})$.

3 Van der Waals interaction

To be specific, we take the bare potential $v(R)$ to be given by the superposition of the short range repulsive and the long range attractive interaction describing the direct vortex-vortex interaction in the extremely decoupled limit $\varepsilon \to 0$,

$$v(R) = v_0 \left(K_0(R/\lambda) - a_{vdw}\phi(R/\lambda)\frac{\lambda^4}{R^4} \right), \tag{22}$$

where $v_0 = 2\varepsilon_o/k_BT$ measures the amplitude of the direct interaction between flux lines, and a_{vdw} determines the strength of the thermal vdW attraction. $\phi(x)$ is a function that smoothly cuts off the power law part for $R \lesssim \lambda$, which we have defined as

$$\phi(x) = \begin{cases} 0, & x \le x_1 \\ \frac{1}{4}\left[1 + \sin\left(\pi\frac{x - (x_1+x_2)/2}{x_2 - x_1}\right)\right]^2, & x_1 < x < x_2 \\ 1, & x \ge x_2 \end{cases} \tag{23}$$

with $x_1 = 1$ and $x_2 = 5$. The choice of the cutoff function, as well as the actual values of x_1 and x_2, is to some extent arbitrary; $x_1 = 1$ is however an obvious choice, and x_2 has to be chosen such that the cutoff is not too sharp and, on the other hand, does not influence the form of the potential in the vicinity of the minimum for those values of a_{vdw} that are physically meaningful [8].

In order to make quantitative predictions for the low-field phase diagram of layered high-T_c superconductors, we identify the parameters introduced above with physical parameters characterizing those systems: the elastic constant is $\tilde{\kappa} = \varepsilon_o/2k_BT$ in the long wavelength regime $\lambda k_z \ll 1$ [9], and the amplitude of the vdW attraction (relative to v_0) is given by $a_{vdw} \approx k_BT/(2\varepsilon_o d \ln^2(\pi\lambda/d))$, where d is the layer spacing [4,8].

Let us quantify these parameters for a specific highly anisotropic material, BiSCCO. This superconductor is characterized by the London penetration depth $\lambda \approx 2000\,\text{Å}$, a Ginzburg-Landau parameter $\kappa \approx 100$, a layer spacing $d \approx 15\,\text{Å}$ and an anisotropy parameter $\varepsilon \approx 1/300$ [9]. Together with the thermal length $L_T \approx 2/T$ cm K, we find for our model parameters the values $\lambda\tilde{\kappa} \approx 10^5/T$ K, $v_0 = 4\tilde{\kappa}$, and $a_{vdw} \approx 2 \times 10^{-5}\,T$ K^{-1}. At $T = 100\,$K, which is of the order of the critical temperature T_c, we finally have $\lambda\tilde{\kappa} \approx 10^3$ and $a_{vdw} \approx 2 \times 10^{-3}$. We want to feed the potential (22) with $\tilde{\kappa}$ and v_0 discussed above into the variational procedure. The London penetration depth λ is chosen to set the length scale in the direction perpendicular to the FLs, *i.e.*, all lengths are measured in terms of λ.

Although the vdW amplitude a_{vdw} is determined by material parameters and the temperature as noted above, we will tune this parameter here in order to find whether a "critical" value a^*_{vdw} exists where the phase transition from the Meissner phase to the mixed phase changes its character from a second order (for $a < a^*_{vdw}$) to a first order transition (for $a > a^*_{vdw}$).

With these parameter values and the potential (22), we have solved the set of self-consistent equations (16–21) numerically for different values of the mean spacing a with fixed FL number $N \times M$ and fixed vertical length $L_\parallel$. In order to speed up computation, the sums over q_z were replaced by integrals.

First, we present the fluctuation matrices (21) as a function of the mean FL distance a. There are 6 fluctuation matrices corresponding to the 6 nearest neighbor vectors given by equation (2). The special choice of these vectors $\mathbf{a}_n$, however, yields only two different matrices, namely

$$\begin{aligned} M^{(1)} &\equiv M_{\mathbf{a}_n} \quad \text{for} \quad n = 1,3,4,6 \quad \text{and} \\ M^{(2)} &\equiv M_{\mathbf{a}_n} \quad \text{for} \quad n = 2,5. \end{aligned} \tag{24}$$

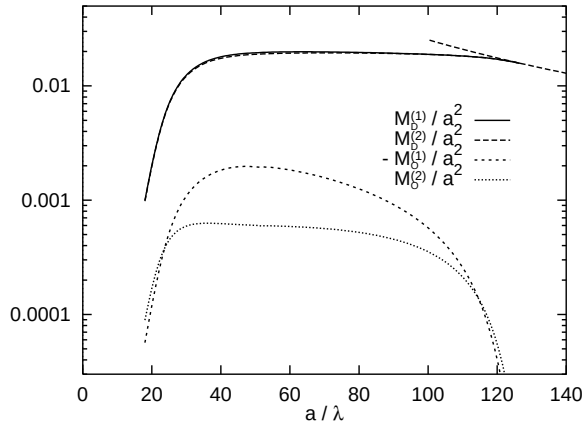

Fig. 2. Fluctuations $M^{(i)}$ divided by a^2, as a function of the spacing a. The two curves $M_D^{(1)}$ and $M_D^{(2)}$ are hardly distinguishable. The vdW amplitude has been set to $a_{vdw} = 10^{-6}$, and the other model parameters to $\tilde{\kappa} = 10^3$, $v_0 = 4 \times 10^3$, $N = M = 100$, $L_\parallel = 5 \times 10^6$, $\Lambda/\pi = 400$. In the upper right corner of the figure, the function $L_\parallel/2\pi^2\tilde{\kappa}a^2$ has been added (*dashed line*) which gives the upper bound for $M_D^{(i)}$, as derived in equation (26).

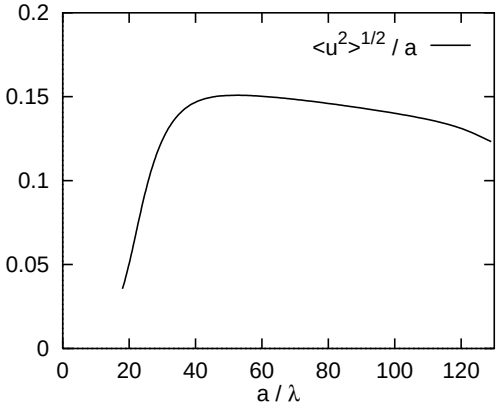

Fig. 3. The fluctuations $(\langle \mathbf{u}^2(0)\rangle)^{1/2}/a$, as a function of a, from the same numerical data as in Figure 2.

With $M^{(1)}$ and $M^{(2)}$ each having two independent entries (the diagonal and off-diagonal terms M_D and M_O, respectively), we have to solve for a total of 4 variables. The implementation made use of a multi-dimensional Newton-Raphson method [11]. Numerical solutions for these four observables are shown as a function of the mean spacing a in Figure 2. The data shown in this figure stems from calculations with the vdW amplitude $a_{vdw} = 10^{-6}$; the corresponding data for higher values of a_{vdw} is not significantly different.

For values of a much smaller than the minimum position of the bare potential (which is at $R_{min} \approx 27\lambda$ for the vdW amplitude chosen here) fluctuations are strongly suppressed by the direct repulsion from the nearest neighbors. The fluctuations grow rapidly around $a \approx 25\lambda$, because in that regime the strong repulsion is neutralized by the vdW attraction. For a large intermediate range, the fluctuations scale almost $\sim a^2$. Note that in that plot, this quadratic scaling would correspond to a horizontal line. Actually, the slope is slightly negative, because the attraction continuously decreases for larger distances. This tendency is most obvious in the plot of the fluctuations

$$\langle \mathbf{u}(0)^2 \rangle = \frac{2}{MNL_\parallel} \sum_{\mathbf{q}} \tilde{K}_D(\mathbf{q}) \tag{25}$$

as a function of a in Figure 3. For $a \gtrsim 150\lambda$, the size of the fluctuations saturates. This is due to the finite system size $L_\parallel$ in the z-direction; in this limit, the contribution of the potential energy to the free energy density is negligible, leaving only the kinetic term. This leads to

$$\begin{aligned} M_{\mathbf{a},D} &= \langle (u_x(\mathbf{x}+\mathbf{a},t) - u_x(\mathbf{x},t))^2 \rangle \\ &\simeq 2 \int_{2\pi/L_\parallel}^{\Lambda} \frac{dq_z}{2\pi} \frac{1}{\tilde{\kappa} q_z^2} \approx \frac{1}{2\pi^2} \frac{L_\parallel}{\tilde{\kappa}}, \end{aligned} \tag{26}$$

where we have assumed that the correlations between neighbors are small and that $L_\parallel \Lambda/2\pi \gg 1$. Finite size effects will hence occur when the mean vortex distance a becomes of the order of $\sqrt{L_\parallel/2\pi^2\tilde{\kappa}}$. In this regime, the off-diagonal terms $M_O^{(1)}$ and $M_O^{(2)}$ vanish due to the effective rotational invariance for each FL in this limit, where the FLs no longer interact with each other.

4 Minimization of the Gibbs free energy

We will now use the effective free energy density $f(a,T) = F(a,T)/L_\parallel N M a^2$, where the free energy $F(a,T)$ is taken to be the minimal value of F^*, to calculate the Gibbs free energy density

$$g(a;\mu,T) = f(a,T) + \mu/a^2 \tag{27}$$

which has to be minimized with respect to the mean FL distance a. For convenience, we have introduced the "chemical potential" $\mu \equiv -\varepsilon_o \tilde{h} \ln \kappa$, where $\tilde{h} = (H - H_{c_1})/H_{c_1}$ is the deviation of the applied magnetic field from the lower critical field.

In Figures 4 and 5, the Gibbs free energy density $g(a;\mu,T)$ as defined in (27) is plotted for two different values of a_{vdw}. For these two values of the vdW amplitude, the transition from the Meissner state to the mixed phase has different characteristics: for $a_{vdw} = 10^{-5}$, the transition is continuous because the minimum position of the potential is continuously shifted to larger values with growing μ, corresponding to a second order phase transition.

For $a_{vdw} = 10^{-4}$, on the other hand, the transition is discontinuous and hence first order, because for μ in the vicinity of μ_c, two minima emerge: one at a finite value of a and the other at $a = \infty$. The magnetization $B \sim 1/a_{min}^2$ as a function of H thus shows a first order transition from the Meissner phase to the mixed phase at a finite magnetization B_v. Hence, the principal result from the study by BG [4] and from the functional RG treatment [8] is reproduced by the variational approach.

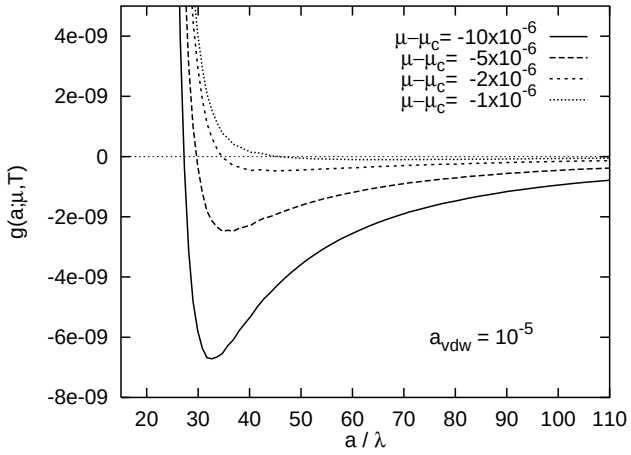

Fig. 4. Gibbs free energy density $g(a;\mu,T)$ for several values of μ, with $a_{vdw} = 10^{-5}$. The data reflects a second order transition from the Meissner phase to the mixed phase.

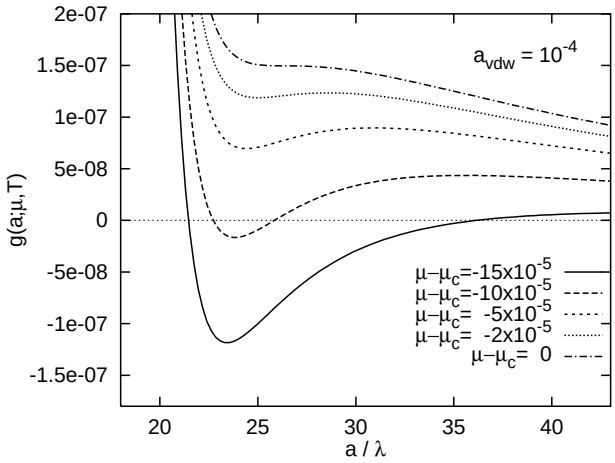

Fig. 5. Gibbs free energy density $g(a;\mu,T)$, now with $a_{vdw} = 10^{-4}$. The figure reflects a first order transition from the Meissner phase to the mixed phase.

The transition is illustrated in Figure 6, where $1/a^2_{min}(\mu)$ is plotted as a function of $\mu - \mu_c$. For each value of a_{vdw}, μ_c has been determined individually such that $g(a;\mu > \mu_c, T)$ has *no* minimum at *finite* a, while it *does* have such a minimum for $\mu < \mu_c$. For $a_{vdw} < a^*_{vdw}$, the magnetic induction is proportional to $\mu - \mu_c$. This scaling arises from the competition between the bare repulsive interaction and the entropic repulsion alone.

For the parameters chosen above, the "critical" value of a_{vdw} separating the two regimes is found to be $a^*_{vdw} \approx 2 \times 10^{-5}$. As stated above, the physical value of the amplitude of the thermally induced van der Waals attraction is of the order $a_{vdw} \approx 10^{-3}$, hence deep in the regime where the transition – according to the variational procedure – is first order. From the data in Figure 6, we read off that the mean separation between FLs just above the transition between the Meissner phase and the mixed phase is $a_{min} \approx 20\lambda$. For BiSCCO, this corresponds to a magnetic induction $B_v \approx 500\,\mathrm{G}/(a_{min}/\lambda)^2 \approx 1.2\,\mathrm{G}$ [9].

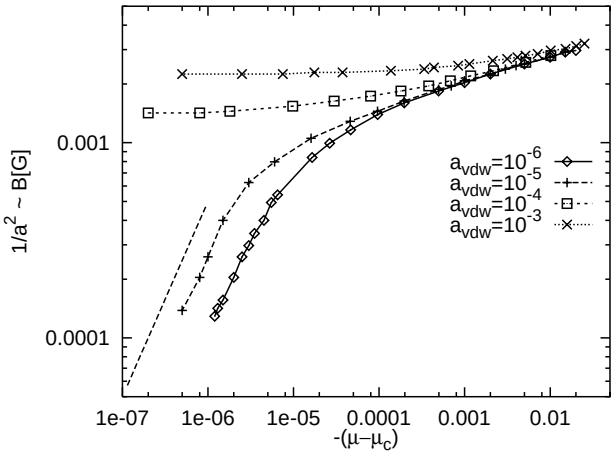

Fig. 6. $1/a^2_{min}$ *versus* $\mu - \mu_c$ for several values of a_{vdw}. In the lower left corner, a (*dashed*) line has been added that shows a linear scaling of the magnetic induction B as a function of $\mu - \mu_c$, revealing the linear scaling of the two lower curves which correspond to the two lowest values of the vdW amplitude. The other curves approach a finite value $1/a^{*2}$ for $\mu \to \mu_c$, thus determining the van der Waals magnetic induction $B_v = \Phi_0/a^{*2}$.

Now, let us face the question whether the basic assumption of the variational approach, *i.e.*, the existence of a regular triangular lattice, is valid for these parameters. This can be checked using the self-consistently determined fluctuations by applying a Lindemann criterion [12,13]. In particular, the elastic structure melts when the displacement between two neighbors becomes

$$\langle (\mathbf{u}_n(z) - \mathbf{u}_m(z))^2 \rangle \geq c_L^2 a^2, \tag{28}$$

where n and m denote two neighboring vortices, a is the lattice constant, and c_L is the heuristically determined Lindemann number. In a recent numerical study on FL lattice melting [14], this number has been found to be $c_L \approx 0.25$, in agreement with usual estimates for vortex lattice melting [9]. With the values represented in Figure 3, we are hence above the lower melting line where the lattice is still stable [15].

In principle, the variational technique can now be used to explore the whole low field phase diagram of layered superconductors, tuning the temperature T. We will restrict ourselves here however to the data shown above, since we do not expect results for the phase diagram that differ qualitatively from those obtained by the functional renormalization group treatment to be discussed below. Instead, we will compare the two techniques and discuss their relative strengths and flaws.

5 Comparison with the functional RG

As noted in the introduction, the problem considered here has recently been addressed by a functional renormalization group calculation [8]. In that approach, the FL interaction potential, equation (22), is renormalized by short

scale thermal fluctuations, analogous to the first RG treatment of the purely repulsive short range FL interaction by Nelson and Seung [13]. The starting point of this technique is the bare Hamiltonian (4) with two interacting FLs. Due to the presence of neighbor vortices in a typical distance a, transverse fluctuations are assumed to be confined to this length scale. Hence, thermal fluctuations are integrated out by means of a momentum shell RG up to this scale, a, applying (nonlinear) recursion relations that are closely related to those that were established in the context of the wetting transition [16]. (Note that this argument applies to the system in a liquid state; in the solid state, the fluctuations are confined to a shorter scale $< c_L a$, as we have seen above.) This procedure renormalizes the interaction potential, leading to an effective potential $V^{\mathit{eff}}(R)$ on the scale a.

For large $a \gg \lambda$, the RG takes us into a region of weak coupling and high vortex densities [13], where the effective Gibbs free energy density simply reads $g(a;\mu,T) = ((z/2)V^{\mathit{eff}}(a)+\mu)/a^2$; here, $z = 6$ is the number of nearest neighbors. Again, $g(a;\mu,T)$ has to be minimized with respect to a in order to obtain the Gibbs free energy density as a function of μ and T, hence on this level the analysis of the phase diagram is identical to that employed within the variational technique. This enables us to directly compare the results of the two approaches.

Returning to the result for B_v obtained above for BiSCCO at $T \approx 100\,\mathrm{K}$, one finds that this value is considerably higher than $B_v^{RG} \approx 0.2\,\mathrm{G}$ as calculated from the functional RG data [8]. This discrepancy is consistent with the fact that the value for a^*_{vdw} determined above is much smaller than the value $a^*_{vdw} \approx 2\times 10^{-3}$ which results from the RG calculations.

The reason for the discrepancy between the two approaches is given by the fact that they include fluctuations up to different maximal scales, as mentioned above. In particular, we have found here that fluctuations are confined to $\sqrt{\langle \mathbf{u}^2\rangle} \approx (0.10\ldots 0.15)a$. Hence, the FLs have a much smaller contact probability than assumed in the RG procedure, and the strong short range repulsion does consequently contribute less to the effective interaction energy, rendering the effective potential more attractive.

This statement can be made more quantitative by adapting the data from the functional RG to the situation where the FLs form a lattice by confining the integration to scales $\leq (1/\eta)\,a$ with a constant $\eta > 1$. An example for the effective interaction V_η^{eff} obtained in this way is shown in Figure 7.

Indeed, the figure reveals that $V_{\mathit{eff}}^{\eta}(a)$ exhibits a global minimum at a finite length scale a for large enough η, while it lacks such a minimum for smaller $\eta \approx 1$. With growing η, the position of the minimum decreases, corresponding to larger values B_v.

Let us compare the results which are shown in Figures 5 and 7 from the variational and the RG approach, respectively, corresponding to the same temperature $T = 100\,\mathrm{K}$ and the same vdW amplitude $a_{vdw} = 10^{-4}$. For this comparison, we determine the appropriate coefficient η from the magnitude $\langle \mathbf{u}(0)^2\rangle$ of the fluctuations, as measured in the variational calculation, with a set to the length a_{min} that corresponds to the position of the free energy minimum. For the present set of parameters, $a_{min} \approx 25\lambda$ (see Fig. 5). The corresponding fluctuations have been determined to be $\langle \mathbf{u}(0)^2\rangle^{1/2} \approx (0.1\pm 0.02)\,a$ (see Fig. 2). A relatively large uncertainty is attached to this value because $\langle \mathbf{u}(0)^2\rangle$ varies rapidly in this regime. Now, we would expect the two techniques to yield comparable results when choosing $\eta \approx 10 \pm 2$. Indeed, the data compare favorably well: $V_\eta^{\mathit{eff}}(a)$ as determined from the functional RG with $\eta = 8$ exhibits a minimum at $a/\lambda = 26 \pm 2$ (see Fig. 7), which is consistent with the value determined by the variational procedure. Modified in this way, both techniques hence predict the same magnetic flux B_v at the transition from the Meissner phase to the mixed phase.

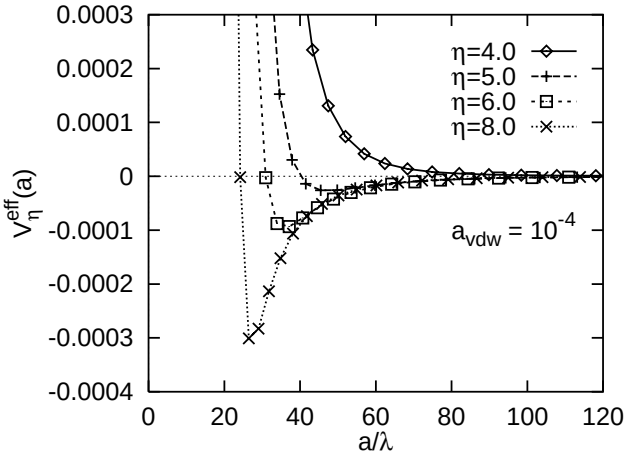

Fig. 7. The effective interaction energy $V_\eta^{\mathit{eff}}(a)$ which results from the functional RG procedure when stopping the integration on the scale a/η. The data result from numerical functional RG calculations with a rescaling factor $b = 1.2$ and $v_0 = 2\times 10^6$, corresponding to the temperature $T = 100\,\mathrm{K}$. The vdW amplitude is set to the values $a_{vdw} = 10^{-4}$.

6 Conclusion

In layered high-T_c superconductors close to the lower melting line H_{c_1} where the mean flux line distance becomes larger than the London penetration depth λ, a long ranged, attractive interaction between the vortices is induced both by thermal or by quenched-in disorder fluctuations which has interesting consequences for the phase diagram of these materials in the regime of low magnetic fields B. In particular, this van der Waals attraction may lead to a first order transition from the Meissner phase to the mixed phase, both for pure and for disordered superconductors.

Restricting ourselves to the pure case, we have established a variational technique that allows for the computation of the van der Waals magnetic induction B_v, which is based on a self-consistent expansion around the regular Abrikosov lattice. We have applied this method to the calculation of B_v in the case of BiSCCO, which is a typical example of a strongly layered high-T_c superconductor.

The results for the low field phase diagram of pure layered superconductors are qualitatively and, to some extent also quantitatively, consistent with the results from a functional RG approach. The latter is the more powerful tool in that it correctly reproduces logarithmic corrections to the leading scaling behavior. It is hence adequate for determining the true asymptotic behavior at the phase transition. The variational technique, on the other hand, has the advantage that it provides an inherent control mechanism as to where to stop the coarse graining process or – in other words – which is the scale on which the effective interaction has to be considered. Furthermore, by self-consistently determining the flux line fluctuations, the results from the variational method can be used to check *a posteriori*, using a Lindemann criterion, whether an expansion around the regular Abrikosov lattice is justified for a given set of physical parameters – which is the basic assumption of the variational calculation. Indeed, this has to be checked carefully since we are working in a part of the phase diagram where the lower lattice melting line B_m and the van der Waals magnetization B_v are of the same order. We note that our result implies that the first order transition is between the Meissner phase and the FL lattice for a large part of the phase diagram – in contrast to previous results that the transition is mainly between the Meissner and the flux liquid phase [8].

We would like to stress that in order to make solid quantitative predictions for the low field phase diagram of BiSCCO, a little more work still has to be done: in particular, one should correctly account for the dispersive nature of the line tension $\varepsilon_l(k)$, which would represent a straightforward extension of our variational approach; also, one could include next-to-nearest neighbour interactions in the procedure.

Finally, we note that the variational approach may be extended to the situation with quenched-in impurities using the replica trick. An advance in this direction could be guided by variational studies of flux lines lattices in high-T_c superconductors in the presence of weak disorder [17,18].

We thank Jan Kierfeld and Thorsten Emig for helpful discussions and the German Israeli Foundation (GIF) for financial support.

References

1. A.A. Abrikosov, Zh. Eskp. Teor. Fiz. **32**, 1442 (1957) [Sov. Phys. JETP **5**, 1174 (1957)].
2. D.R. Nelson, Phys. Rev. Lett. **60**, 1973 (1988).
3. D.S. Fisher, M.P.A. Fisher, D.A. Huse, Phys. Rev. B **43**, 130 (1991).
4. G. Blatter, V. Geshkenbein, Phys. Rev. Lett. **77**, 4958 (1996).
5. E.H. Brandt, R.G. Mints, I.B. Snapiro, Phys. Rev. Lett. **76**, 827 (1996); R.G. Mints, I.B. Snapiro, E.H. Brandt, Phys. Rev. B **55**, 8466 (1997).
6. V. Geshkenbein, G. Blatter, *Van der Waals Attraction Between Vortices in HTSC*, Proceedings of the 21st Int. Conference on Low Temperature Physics, Prague, August 8–14, 1996, Czech. J. Phys. **46**, 1827 (1996).
7. S. Mukherji, T. Nattermann, Phys. Rev. Lett. **79**, 139 (1997).
8. A. Volmer, S. Mukherji, T. Nattermann, Eur. Phys. J. B (to appear, 1998), preprint `cond-mat/9802090`.
9. G. Blatter, M.V. Feigel'man, V.B. Geshkenbein, A.I. Larkin, V.M. Vinokur, Rev. Mod. Phys. **66**, 1125 (1994).
10. P.M. Chaikin, T.C. Lubensky, *Principles of condensed matter physics* (Cambridge University Press, Cambridge, 1995).
11. W.H. Press *et al.*, *Numerical Recipes in C*, 2nd edn. (Cambridge Univ. Press, 1992).
12. F.A. Lindemann, Z. Phys. **11**, 609 (1910).
13. D.R. Nelson, H.S. Seung, Phys. Rev. B **39**, 9153 (1989).
14. H. Nordborg, G. Blatter, preprint `cond-mat/9803041` (1998).
15. Note that in order to calculate the exact lower melting line $B_m(T)$ for highly anisotropic superconductors, one has to account for the full dispersive nature of the line tension $\varepsilon_l(k_z)$ [G. Blatter, V. Geshkenbein, A. Larkin, H. Nordborg, Phys. Rev. B **54**, 72 (1996)]. Since the short scale modes are softer, the real melting line $B_m^{el}(T)$ is somewhat larger than the values obtained with our simpler model.
16. R. Lipowsky, M.E. Fisher, Phys. Rev. Lett. **57**, 2411 (1986); Phys. Rev. B **36**, 2126 (1987).
17. M. Mézard, G. Parisi, J. Phys. I France **1**, 809 (1991).
18. T. Giamarchi, P. Le Doussal, Phys. Rev. Lett. **72**, 1530 (1994); Phys. Rev. B **52**, 1242 (1995).